Unequivocal Experimental Evidence of the Relationship between Emission Energies and Aurophilic Interactions.

Alexander J. Blake[1], Rocío Donamaría[1,2], Vito Lippolis[3], José M. López-de-Luzuriaga[2]*, Miguel Monge[2], María E. Olmos[2], Alexander Seal[1], Julia A. Weinstein[4].*

[1]School of Chemistry, University of Nottingham, University Park, Nottingham NG7 2RD, UK.

[2]Departamento de Química, Universidad de La Rioja, Centro de Investigación en Síntesis Química (CISQ), Complejo Científico-Tecnológico, 26004-Logroño, Spain.

[3]Dipartimento di Scienze Chimiche e Geologiche, Università degli Studi di Cagliari, S.S. 554 Bivio per Sestu, 09042 Monserrato (CA), Italy.

[4]Department of Chemistry, University of Sheffield, Sheffield S3 7HF, UK.

KEYWORDS. Aurophilicity, Luminescence, X-Ray Diffraction, High pressure

ABSTRACT. In this paper we describe experimental evidence of the change in emission energy as a function of gold-gold distance. We have employed a luminescent complex exhibiting an aurophilic interaction, which is weak enough to allow its length to be modified by external pressure, but rigid enough to confer structural stability on the complex. By determining the crystal structures and emission characteristics over a range of pressures, we have identified an exponential relationship between the wavelength of the emitted light and the metal-metal distances under pressure. This result can be indirectly related to the repulsive branch of the fitted function representing the energy of the system at different gold-gold distances. The relativistic nature of gold appears to play an important role in the behaviour of this complex.

INTRODUCTION

The pursuit of a direct relationship between weak interactions and emission wavelengths is not a new challenge. Historically, the preferred candidates to investigate it were square-planar Pt(II) and linear Au(I) closed-shell metal complexes, and more recently also Ag(I) ones, because they usually display unsupported metal-metal interactions with a great variety of metal-metal distances, as has been summarized by Pyykkö, Schmidbaur et al. in highly cited reviews.[1,2] This variety has even been found in the very unusual E/Z-isomerism between two isomers of complex $[Au(C_6Cl_5)_2Ag([9]aneS_3)]_2$ recently reported by our laboratory.[3] Indeed, these interactions are considered in most cases to be responsible for the emissions that appear in these complexes;[4,5] consequently, any variation of the metal-metal distances should lead to a bathochromic or

hypsochromic shift of the emissions with reduced or lengthened metal-metal distances, respectively. Despite the apparent simplicity of the reasoning, all attempts to find such a relationship for different gold or platinum complexes have been historically fruitless, mainly because of the difficulty of finding a suitable set of complexes for comparison. For example, in the case of the studies with different gold(I) salts, the different anions, cations or ligands produced conformational changes, which altered the molecular packing, or even changed the characters of emissions, leading to results which did not provide any insight.[6-9]

An alternative strategy, carried out mainly with platinum(II) and gold(I) complexes, consisted of subjecting emissive complexes to high pressures. This is the case for the extensively studied family of complexes $[Pt_2(POP)_4]^{4-}$ (POP = $H_2P_2O_5$), but increasing pressures frequently provoked new excimer emissions, disappearance of bands, unexpected changes in intensities or fine structures.[10-13] In the case of $M[Au(CN)_2]$ salts, the shifts of the emissions under pressure depend on the different compressibility of the metal-metal interactions within a two-dimensional network.[14-16] Similar problems also appear in complexes of stoichiometry $[Au_2(dtc)_2]_n$ (dtc = dithiocarbamate) or $[Au_3(\mu_2\text{-pyrazolato-}N,N')_3]$, in which the multiple Au···Au interactions present give rise to new bands, making an unequivocal correlation impossible.[17,18]

Thus, the problem lies in finding a candidate system for this study that fulfils an exacting series of requirements:

1) The complete study should be done on a single complex, avoiding any variation of counterions or ligands, which could affect its electronic structure.

2) The ideal intermetallic interaction should be not imposed by the structural architecture (*i.e.* it should not be enforced by bridging ligands) and the involved atoms should be able to move freely and significantly when the pressure is varied.

3) The complex must be isolated from others in the crystal lattice to preclude the formation of new interactions between different units under pressure with the concomitant appearance or quenching of emission bands.

4) The study should give information about the crystal structure at each pressure point in order to identify possible changes of phase that affect the molecular packing or the metal-metal distances, at the same temperature to avoid thermal effects; finally, the crystals must be insoluble in the chosen pressure-transmitting medium in order to avoid solvent effects or the loss of the crystal by dissolution.

5) Ideally, in order to avoid structural or electronic changes that could affect the energy of the emission, the main change expected under compression should be a progressive variation of the studied metal-metal distance, leaving the rest of the structural parameters almost unchanged.

Herein we describe high pressure luminescence studies on the complex *E*-$[Au(C_6Cl_5)_2Ag([9]aneS_3)]_2$ representing the first experimental evidence of an unequivocal relationship between Au···Au distances and emission energies for a single molecule. This relationship can be related to the repulsive branch of the fitted curve that represents the potential energy of the system at different gold-gold distances.

RESULTS

CRYSTALLOGRAPHIC STUDY

The diffraction experiment on the *E*-isomer enclosed in a diamond-anvil cell (DAC) at ambient pressure shows a crystal system, space group and unit cell dimensions different from those obtained previously,[3] suggesting that a new phase of the *E*-isomer has been obtained (**Table S1**). Comparison of the powder patterns of the two phases (**Figures S1**-**S2**) confirm that they are indeed different. The crystal structure of the new phase (β-*E*) consists of two $[Au(C_6Cl_5)_2]^-$ anions and two $[Ag([9]aneS_3)]^+$ cations, leading to a heteropolynuclear Ag···Au···Au···Ag system, as in the original crystal structure. The most important difference between the two phases lies in the number of molecules present in the crystallographic asymmetric unit; the new β-*E* phase contains two molecules of $[Au(C_6Cl_5)_2Ag([9]aneS_3)]$, while the original phase (α-*E)*, contains only one. Since the main difference between the data collection at high pressure and at the original structural determination is the temperature at which the experiments were carried out, the effects of temperature on the *E*-isomer were investigated by means of variable-temperature experiment (See SI).

Effects of pressure on unit cell parameters.

Between 3.6 and 6.2 kbar, increasing pressure leads to a crossover of the *a* and *b* unit cell dimensions, accompanied by a change in the *c* unit cell dimension and a volume increase, indicative of a phase transition where the space group changes from *P*-1 to *C*2/*c* (**Table S1)**. A visual comparison doing a molecular overlay (**Figure S3**) revealed that the molecular structure is the same in the two phases. The monoclinic phase has the same space group and very similar unit cell dimensions to the phase we originally identified for *E*-$[Au(C_6Cl_5)_2Ag([9]aneS_3)]_2$,[3] and

comparison of calculated powder patterns showed them to be closely similar, confirming that the phase observed at 6.2 kbar is indeed the original α-*E*-phase (**Figure S4**).

Moreover, we have studied the reversibility of the high-pressure experiment by applying stepwise reductions in pressure. The dependence of the unit cell dimensions upon pressure reduction follows in reverse the same trend as that observed during the pressure increase, suggesting that there is no hysteresis and establishing that the effects of compression are completely reversible. When the pressure was reduced the β-*E* phase reappeared at 5.2 kbar, confirming that the phase transition is fully reversible and occurs in the range 5.2–6.2 kbar.

Effects of pressure on the molecular geometry.

At pressures above 21.3 kbar, disorder affects almost the whole structure (**Fig. S8**): the entire $[Ag([9]aneS_3)]^+$ cationic fragment is disordered, as are both of the pentachlorophenyl ligands (for more details see SI). The fact that the only atoms not affected by disorder are the gold(I) centres allows us to do an in-depth study of the variation of the Au···Au distance with pressure and the associated effects on the optical properties of the complex.

The decrease in this distance with pressure can be fitted to an exponential expression, with the rate of contraction decreasing towards higher pressures: for example, the initial Au···Au distance decreases by 7.0% between ambient pressure and 13.5 kbar, but only by 12.7% between 13.5 and 149.4 kbar, indicating that as the gold(I) centres approach each other, ever-higher pressures are necessary to get shorter Au···Au distances. Upon decompression, the Au···Au interactions show the reverse trend to that observed during compression with no lag, indicative of the absence of hysteresis (**Table S3** and **Fig. 1**).

At this point, it is important to note that the Au···Au interaction lies parallel to the *a* axis, which is consistent with the larger contraction (14.4%) of this axis. A similar phenomenon was observed in a previous study.[19]

Throughout the compression of the crystal, distinct colour changes were readily perceptible to the human eye. At ambient pressure the crystal is green, but between 13.5 and 21.3 kbar its colour changes to yellowish-green and between 34.3 and 48.7 kbar it turns yellow (**Fig. 2**). The Au···Au distance at ambient pressure is 3.3962(7) Å, decreasing to 3.0300(15) Å at 34.3 kbar where the crystal is yellow. The latter value is very close to that of 3.0396(3) Å previously reported by some of us for a yellow crystal of the *Z*-$[Au(C_6Cl_5)_2Ag([9]aneS_3)]_2$ isomer at ambient pressure.[18] It was previously suggested that the differences in the Au···Au distances or the relative positions of the $[Ag([9]aneS_3)]^+$ cationic fragments could be the responsible for the different optical properties of the two isomers. Given that the position of the cationic fragment with respect to the Au···Au direction does not change when the pressure is varied, the Au···Au interaction distance appears to determine the colour of the crystal. The crystal is orange above 53.7 kbar, becoming dark orange at the highest pressures, probably due to the increasing density of the crystal. It is worth noting that the Au···Au distance decreases to 2.758(11) Å at 149.4 kbar, which is the shortest Au···Au distance so far described in high-pressure crystallographic studies, and is even shorter than twice the radius obtained from the cubic crystals of gold metal ($2 \times r_{Au}$ = 2.88 Å) and very close to twice the covalent radius of gold ($2 \times r_{cov,Au}$ = 2.72 Å).[20]

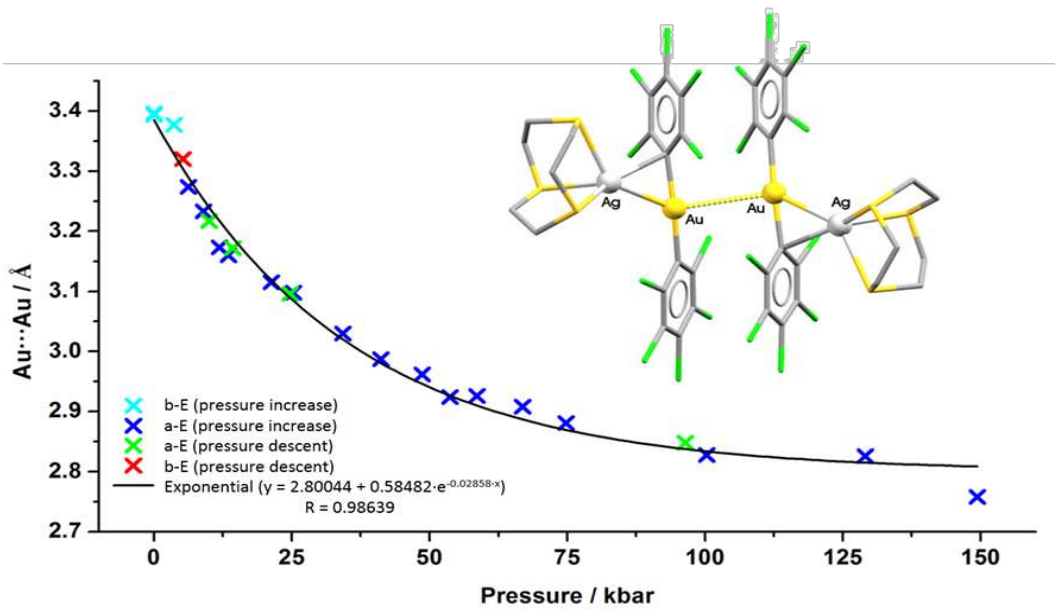

Figure 1. Molecular structure and pressure dependence of the Au···Au distance for the *E*-$[Au(C_6Cl_5)_2Ag([9]aneS_3)]_2$.

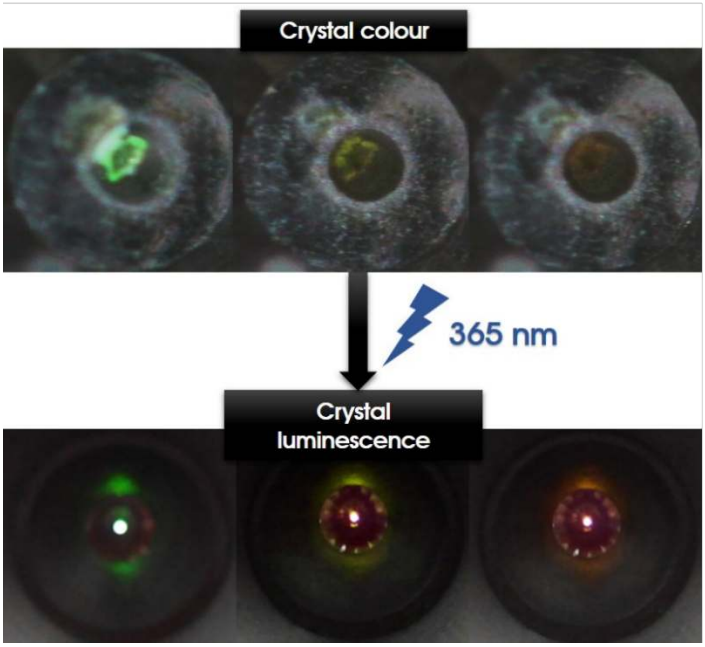

Pressure (kbar)	Emission Energy (nm)	Au···Au (Å)
0	518	3.40
15	524	3.17
30	540	3.04
38	544	3.00
59	558	2.92
72	574	2.88
77	576	2.86
104	601	2.82

Figure 2. Left: (top) Crystal colour at ambient pressure (green), between 34.3 and 48.7 kbar (yellow) and above 53.7 kbar (orange). (bottom) Crystal luminescence at 14.7 kbar (green), at

38.3 kbar (yellow) and at 77.1 kbar (orange). Right: Emission properties and Au···Au distances at different pressures.

Over the total pressure range studied, the Au···Au distance decreases by 18.8%, the largest pressure-induced contraction recorded to date for this type of interaction.

Finally, it is noteworthy that the colour change is reversible upon decompression, such that by 5.25 kbar the crystal has recovered its initial green colour, as well as the Au···Au distance expected at this pressure.

PHOTOPHYSICAL PROPERTIES AT DIFFERENT PRESSURES AND AMBIENT TEMPERATURE.

E-[Au(C_6Cl_5)$_2$Ag([9]aneS_3)]$_2$ shows a single emission band at room temperature (518 nm; ex. at 366 nm) and at 77 K (518 nm; ex. at 352 nm), with a large Stokes shift and a lifetime in the microsecond range (2.5 μs), suggesting that the emission has its origin in a phosphorescent gold-centred emissive process.[3] Moreover, this complex shows an almost quantitative quantum yield at room temperature, which together with the lifetime value gives a very high radiative constant (k_r = 3.2 x 10^5 s^{-1}), making it an exceptional candidate to detect its emissive properties under very challenging instrumental conditions. The challenge arises because of the need to detect luminescence from an irradiated single crystal of very small size, suspended in ethanol/methanol as the pressure-transmitting medium (PTM) and enclosed in a diamond-anvil cell (DAC), which permits only very limited access to the crystal *via* apertures of only 0.2 mm (see SI). However, this complex fulfils the requirements set out previously for an experiment to establish a relationship between emission energy and metal-metal distances under different pressure conditions.

The progressive changes in colour visible to the human eye, from green (ambient pressure) to orange (above 53.7 kbar), are much more evident when the complex is exposed to UV light (**Figure 2**). Irradiation with monochromated laser light of λ = 365 nm at different pressures affords emission spectra displaying maxima from 518 nm (0.001 kbar) to 601 nm (103.5 kbar), corresponding to a red shift of ca. 2670 cm^{-1}, which represents a wide energy range that allows us to discern the emissive changes under pressure.

Traditionally, these emissions changes are assigned to arise from a linear dependence of the destabilization/stabilization of the frontier HOMO/LUMO on the shortening of the Au···Au distance, as a consequence of a greater overlap of the filled $5d_{z^2}$ and empty $6s/6p_z$ orbitals (see **Figure 3**). This intuitive and commonly-reported representation considers only the energies of the ground state frontier orbitals, ignoring the energies of these orbitals in the excited state from which the emission is produced, and where the destabilization/stabilization of the frontier orbitals could adopt a different ratio.

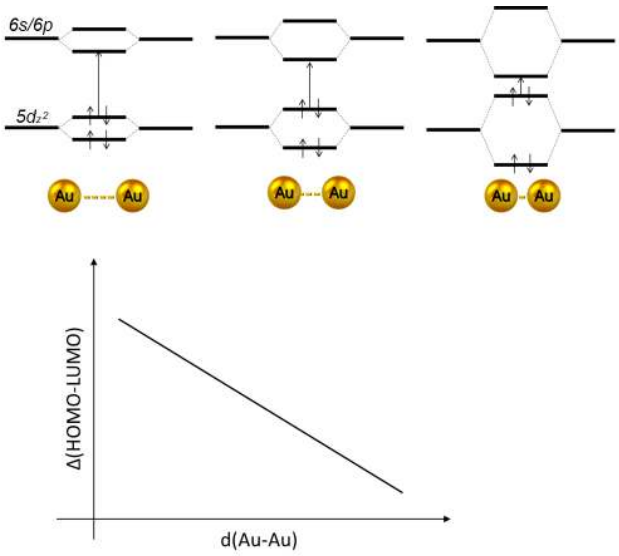

Figure 3. Conventional representation of the HOMO-LUMO gap variation with decreasing Au···Au distance.

Very surprisingly, when we represent the emission energies vs. the Au···Au distances at the different pressures we obtain an exponential decrease of the emission energy with decreasing metal-metal distances (**Figure 4**). This result differs from those previously reported by different groups in which a straight line (lower energy values with decreasing Au···Au distances, see above) was the *a priori* expectation,[5] or more surprisingly, when the opposite trend was obtained.[6,8]

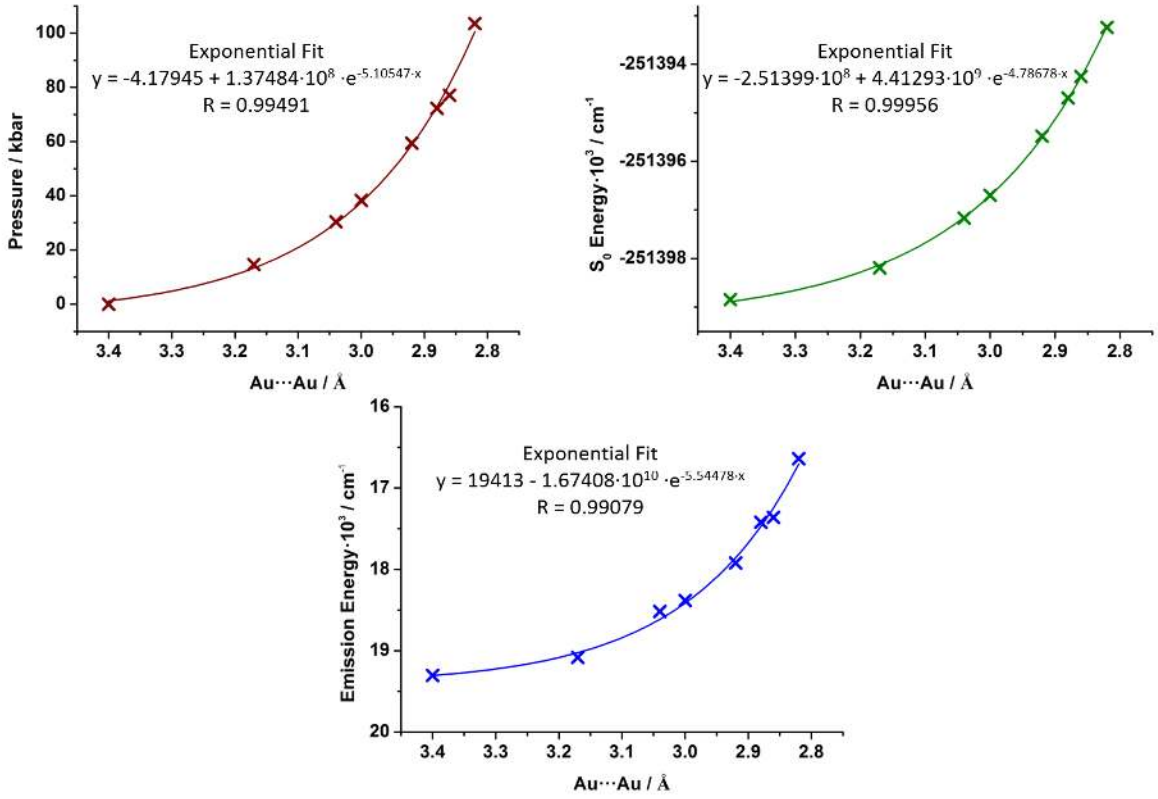

Figure 4. Top-left: pressure *vs* Au···Au distance. Top-right: DFT-computed electronic energy of the ground state S_0 *vs* Au···Au distance. Bottom: emission energy *vs* Au···Au distance.

As mentioned above, when we represent the applied pressure versus the Au···Au distance we also obtain an exponential representation that shows the expected decrease in the Au···Au distance with increasing pressures.

Likewise, when we represent the DFT-computed single point energies of the molecule at different Au···Au distances, as expected, we obtain an exponential dependence which represents the repulsive branch of the potential energy curve of the molecule as a function of Au···Au distance. Very significantly, the shape obtained for this curve matches those found for emission energy *vs* Au···Au distance and pressure *vs* Au···Au distances (**Figure 4**).

These results indicate that the four parameters (experimental Au···Au distance at different pressures, energy of the emissions, computed S_0 energy and applied pressure) are directly related (see SI). Indeed, when we represent the relations between the different *y* axes in the previous graphics as follows: (*i*) the emission energies *vs* the ground state S_0 energies; (*ii)* the applied pressure *vs* the emission energies; or (*iii*) ground state S_0 energies *vs* applied pressure, we obtain linear fits in all cases (*R* of 0.989, 0.994 and 0.994, respectively; **Figure 5**), which validate the assumption of a direct relationship between all the variables. *In other words, an applied pressure reduces exponentially the Au···Au distance, which in turn increases the energy of the system, and this potential energy is linearly related to the energy of the luminescent emission which results from that interaction*.

Effectively, if we represent in a three-dimensional space the values of pressure, emission energies and ground state S_0 energies for each experimental Au···Au distance, we obtain a straight line, confirming the direct relationship among these three parameters. This is a very important finding because it provides direct experimental evidence about the repulsive branch of the fitted

curve that represents the potential energy of the system at different gold-gold distances, which mathematically is considered straightforward, but for which experimental evidence has previously been lacking.

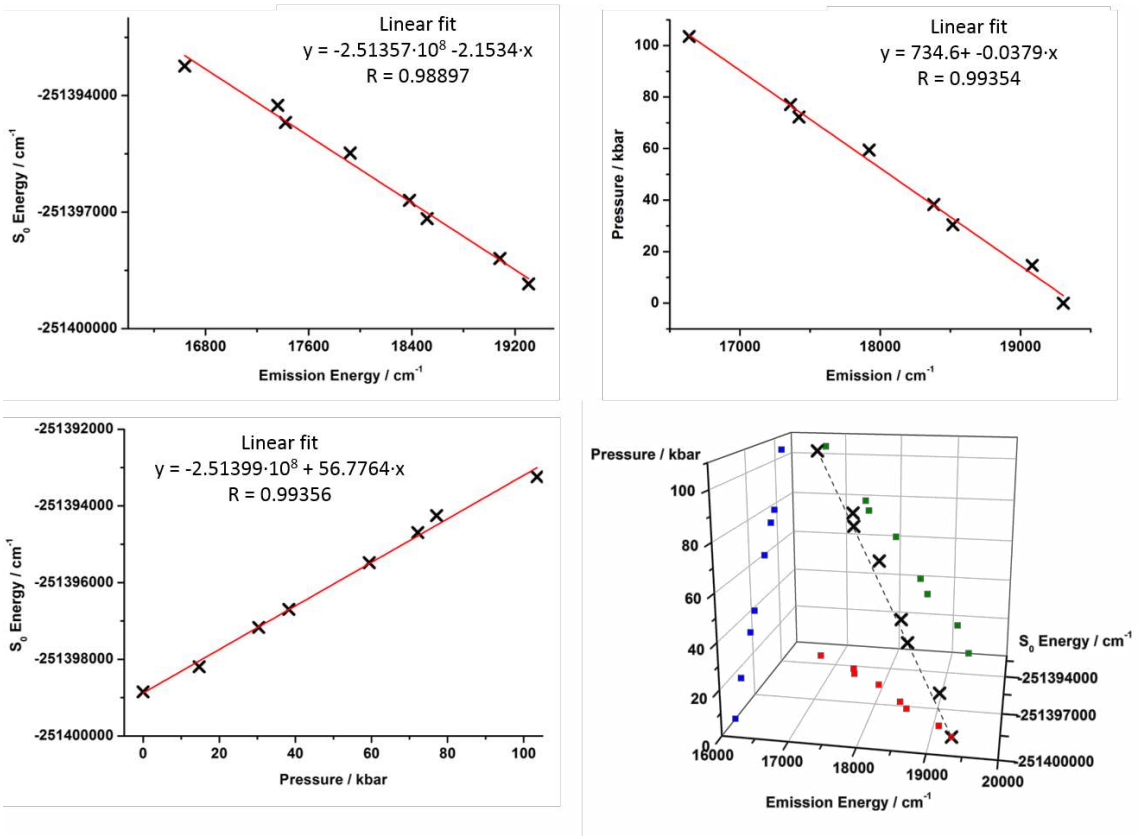

Figure 5. Top-left: S_0 energy *vs* emission energy. Top-right: Pressure *vs* emission energy. Bottom-left: S_0 energy *vs* pressure. Bottom-right: 3D representation of S_0 energy (x) *vs* emission energy (y) *vs* pressure (z) (black crosses). Projection on the XY plane = emission energy *vs* S_0 energy (red squares). Projection on the XZ plane = pressure *vs* S_0 energy (blue squares). Projection on the YZ plane = pressure *vs* emission energy (green squares).

DISCUSSION OF RESULTS.

In principle, predicting the response of a molecule to pressure increments is complicated. In this case, of all the structural changes that this molecule could potentially undergo when subjected to extreme external pressures, we found that the main deformation caused at almost every increment of pressure was a reduction in the Au···Au distance that follows an exponential trend. This has solved the potentially intractable problem of displacement over a ground state potential energy surface in any direction, as a consequence of the multiple variation of bond lengths and angles under pressure. Instead, we find a direct line to higher energies through the modification of only one parameter, namely the Au···Au distance. This converts a three-dimensional walk over the potential energy surface into a two-dimensional one (energy vs. Au···Au distance), in accordance with the most common representation of a Morse potential function drawn in many papers and textbooks. Thus, we can assume that the minimum energies of the ground states at the shorter gold-gold distances observed at increased pressures lie on the repulsive part of the Morse potential of the ground state, computed at ambient pressure as a function of the gold-gold distances (**Figure 6: left**).

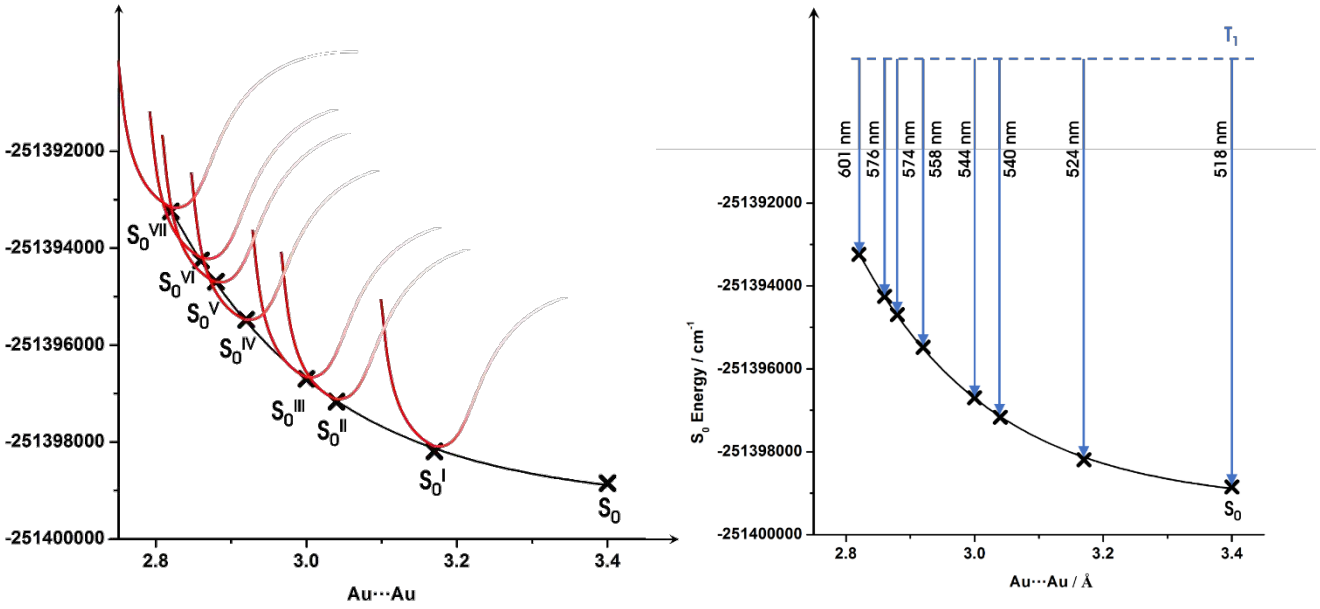

Figure 6. Left: calculated S_0 energy at DFT level of theory *vs* Au···Au distance (black). Representation of the S_0 energy at different pressures (red). Right: Calculated S_0 energy at DFT level of theory *vs* Au···Au distance (black). Minimum energy of T_1 at all S_0 Au···Au distances and the corresponding emission wavelength (blue).

This exponential representation of the S_0 energies upon reduction of the gold-gold distance has a shape similar to the tendency obtained when the energies of the emitting lights of the crystal (irradiated with a 365 nm laser) at different pressures are represented, in contrast to what it was proposed in earlier publications. This situation probably arises from the fact that the Au···Au distance is the main and progressive structural distortion observed under increasing pressure. Nevertheless, our studies raise a question without an obvious answer: *Why does the variation of the emission energies with shortening gold-gold distances follow an exponential trend similar to those for the potential energy of the ground state or the metal-metal distances under increasing pressure?*

At this regard, it is generally assumed that the compression energy is not dissipated as heat, instead increasing the internal energy and provoking a significant perturbation of the system which influences its electronic states. Thus, the simplest picture considers that compression would lead to an increasing overlap of the orbitals of adjacent atoms, thereby reducing the energy gap between the ground and excited electronic states to a degree which is strongly dependent on the orbital type.[21]

In the case of the ground state in our system, increments of pressure and thereby internal energy should lead to higher ground state S_0 energies, which follow the exponential function described previously. However, the role of the excited states in high pressure experiments remains a fundamental issue that is far from being fully understood.

Taking into account that the energy changes of the emitting light follow an exponential trend similar to the S_0 energy destabilization with increasing pressure (reducing Au···Au distances) as indicated previously, the luminescence measurement results seem to suggest that the pressure would not significantly affect the energy of the excited state in this case. In fact, the DFT optimization of the lowest triplet excited state for this complex shows a dramatic shortening of the Au(I)···Au(I) distance to 2.747 Å. This value is even shorter than the shortest experimental Au···Au distance obtained at the highest applied pressure in the ground state (2.758 Å at 149 kbar). Therefore, we could assume that the electronic excitations at any of the studied pressures would relax to a similar constrained lowest triplet excited state (**Figure 6: right**).

Another possible explanation for the emissive behaviour observed with increasing pressures would arise from the usual explanation of a destabilization of the ground state and a stabilization of the excited state (vertical contribution). This change could also lead to variations along the

configuration coordinates because of their possibly different compressibility (horizontal contribution). In addition, the distortion of one or both surfaces would change the individual vibrational energy levels and wavefunctions at each pressure. Nevertheless, the differences in energy at each point should perfectly match those of the exponential behaviour observed and, at the same time, they should coincide perfectly with the exponential functions that match the shortening of the Au···Au distance and the ground state energy, a situation that in light of the results discussed above seems highly unlikely due to the large number of energy coincidences which would be involved.

As is well known, relativistic effects play a fundamental role in the intermetallic interactions in heavy metals, reaching a maximum for gold.[1] Therefore, we have estimated the role played by these relativistic effects in the studied range of intermetallic Au···Au distances. The computed energies of the ground state for the studied model system using non-relativistic pseudopotentials for the gold atoms shows that, upon decreasing the Au···Au distances, the potential energy increases to values higher than those described above with quasirelativistic pseudopotentials. Indeed, the representation of the difference between non-relativistic and pseudorelativistic potential energy versus the Au···Au distance also follows an exponential function (**Figure S19**), what suggests an exponential increase of the relativistic effects for gold(I) due to the closer approach of the electrons to the nuclei caused by the compression of the electronic clouds at extreme pressures. In addition, the representation of the energy of emission versus the potential energy of the ground state using non-relativistic pseudopotentials does not follow a straight line as obtained above, underlining the importance of the relativistic effects in the description of the emissive properties.

CONCLUSIONS

In conclusion, the application of high pressure has been shown to be a very effective method for manipulating the Au···Au distance in *E*-[Au(C_6Cl_5)$_2$Ag([9]aneS_3)]$_2$. Its combination with X-ray diffraction studies has enabled a precise determination of the interactions between these centres and, concomitantly, the luminescence emission and the energy value at each distance. In addition, since we regard the Au···Au interaction as the only parameter responsible for the emissive behaviour, we could extrapolate this result to other complexes or systems featuring the same interaction.

METHODS

Synthesis.

The isomer *E*-[Au(C_6Cl_5)$_2$Ag([9]aneS_3)]$_2$ was prepared according to literature procedures.[3] It was recrystallized using solvent diffusion methods: the complex (5.0 mg) was dissolved in THF (2 mL) and the solution filtered; hexane was then layered on top and the solution allowed to stand for 1 or 2 days to yield green prismatic crystals.

Crystallographic measurements.

Variable-temperature single-crystal X-ray diffraction experiments were performed on a Rigaku Oxford Diffraction SuperNovaII diffractometer equipped with a microfocus sealed-tube source focussing mirror-monochromated Cu-*K*α radiation (λ = 1.54148 Å) and with an Oxford Cryosystems Cryostream open-flow cryostat. The crystal was mounted in a Fomblin film on a MiTeGen MicroMount™ and datasets were collected at 298, 280, 260, 250, 240, 230, 220, 210, 200, 180, 150 and 130 K; the ramp rate between these temperature points was 360 K/h.

High-pressure single crystal X-ray diffraction experiments were carried out using a Merrill-Basset diamond anvil cell (DAC) [opening angle 38° (2θ), culet faces 600 μm, WC backing plates, 100 x 100 x 0.02 mm tungsten gaskets, gasket hole diameter of 0.2 mm]. Three different crystals of *E*-[Au(C_6Cl_5)$_2$Ag([9]aneS_3)]$_2$ of sizes 1: 0.12 x 0.06 x 0.03 mm, 2: 0.16 x 0.12 x 0.06 mm, 3: 0.09 x 0.08 x 0.01 mm, were investigated. Each crystal was loaded into the DAC, along with a small ruby sphere as a pressure calibrant for ruby fluorescence measurements[22] and methanol/ethanol (4:1) as the pressure-transmitting medium (PTM). Diffraction measurements were performed on a Rigaku SuperMovaII diffractometer equipped with a microfocus sealed-tube source focussing mirror-monochromated Mo-*K*α radiation (λ = 0.71073 Å) detected with an Eos CCD area detector. Data collections were carried out at ambient pressure and subsequently at 3.65, 6.24, 9.03, 11.9, 13.5, 21.3, 25.3, 34.3, 41.2, 48.7, 53.7, 58.6, 66.9, 74.8, 100.3, 129.1 and 149.4 kbar; during decompression data were collected at 96.4, 55.6, 24.7, 14.3, 10 and 5.25 kbar. Prior to the loading of the PTM, framesets were collected on crystals inside the DAC at ambient pressure and temperature to provide a good starting model for structure refinement.

Unit cell refinement and data reduction were performed using *CrysAlisPRO*.[23] Multi-scan absorption corrections were applied using SADABS.[24] Structure solution and refinement were implemented through OLEX2:[25] structures were solved using the Patterson method or by model transfer and structures were refined to convergence using least squares using SHELXL.[26] Due to the inherent low completeness of the diffraction data resulting from the presence of the diamond anvil cell, SHELXL-compatible restraints and constraints were required in some cases. Within the [9]aneS_3 ligand the C–C bonds were restrained to 1.52(2) Å and the C–S bonds to 1.82(2) Å. In some cases, the aromatic C–C bonds were restrained to 1.39(2) Å; in other cases, similarity restraints with a standard uncertainty of 0.01 Å were applied to chemically-equivalent C–C and

C–Cl bonds of the pentachlorobenzene ligands. In some structures, this was not effective and the six-membered rings were constrained to be regular planar hexagons. Occasionally, a planarity restraint with a standard uncertainty of 0.05 Å was applied to the pentachlorobenzene ligand. In all cases, rigid-body restraints with a standard uncertainty of 0.02 Å were applied to the whole structure. With the degradation of the crystal quality at very high pressure, ISOR restraints and EADP constraints[25] were applied as required.

At pressures in excess of 21.3 kbar, extensive whole-molecule disorder was identified, requiring the application of a two-component disorder model along with appropriate SHEXL restraints and constraints.

Luminescence measurements.

We prepared four different DACs, each with a single crystal of *E*-[Au(C_6Cl_5)$_2$Ag([9]aneS_3)]$_2$, ruby sphere and PTM, following the same procedure as for the crystallographic measurements. The luminescent measurements were carried out at pressures of 14.7, 30.4, 38.3, 43.3, 59.4, 72.2, 77.1 and 103.5 kbar. The emission spectra were recorded with a Jobin-Yvon Horiba FluoroMax-4 spectrofluorometer with a fibre optic cable transferring the light from the sample to the detector.

Computational Details.

All calculations were carried out using the Gaussian 09 package.[27] DFT calculations were carried out using the PBE functional.[28] The following basis set combinations were employed for the metals Au and Ag: the 19-VE pseudorelativistic pseudo-potentials or the non-relativistic 19-VE pseudopotentials from Stuttgart and the corresponding basis sets augmented with two f

polarization functions were used.[29] The heteroatoms were treated by Stuttgart pseudopotentials,[30] including only the valence electrons for each atom. For these atoms double-zeta basis sets of ref 30 were used, augmented by d-type polarization functions.[31] For the H atom, a double-zeta and a p-type polarization function were employed.[32] The model system used for the calculations was built from the X-ray diffraction structure of complex *E*-[{Au(C_6Cl_5)$_2$}$_2$Ag([9]aneS_3)]$_2$ In a first stage, we fully optimised the tetranuclear models *E*-S_0 and *E*-T_1, which correspond to the ground-state and first triplet-excited state for the complex. The single point energy of the ground state at different pressures were calculated from the optimized ground state model only varying the gold-gold distances.

ASSOCIATED CONTENT

Supplementary Information. Supplementary Information includes Materials and methods; unit cell data; calculated X-ray powder patterns; pressure dependence of structural parameters and photophysical properties. CCDC 1848921-1848944, 1849967 and 1899134 contain the supplementary crystallographic data for this paper: these data can be obtained free of charge from the Cambridge Crystallographic Data Centre via www.ccdc.cam.ac.uk/structures.

AUTHOR INFORMATION

Corresponding Author

* E-mail for J.M.L-de-L.: josemaria.lopez@unirioja.es

* E-mail for A.J.B.: alexanderjohnblake@outlook.com

ACKNOWLEDGMENTS

R. D., J. M. L.-d.-L., M. M., and M. E. O. thank the D.G.I. MINECO/FEDER (Project No. CTQ2016-75816-C2-2-P (AEI/FEDER, UE)). R. D. acknowledges CAR for a FPI grant. A.J.B. thanks EPSRC (UK) for the funding of a diffractometer. V.L. thanks the Fondazione di Sardegna (FdS) and Regione autonoma della Sardegna (RAS) (Progetti Biennali di Ateneo FdS/RAS annualita 2016).

REFERENCES

(1) a) Pyykkö, P. Strong Closed-Shell Interactions in Inorganic Chemistry, *Chem. Rev.*, ***97***, 597–636 (1997). b) Pyykkö, P. Relativity, gold, closed-shell interactions, and $CsAu{\cdot}NH_3$. *Angew. Chem. Int. Ed. Engl.*, ***41***, 3573–3578 (2002).

(2) a) Schmidbaur, H; Schier, A. A briefing on aurophilicity. *Chem. Soc. Rev.*, ***37***, 1931–1951 (2008). b) Schmidbaur, H; Schier, A. Aurophilic interactions as a subject of current research: an up-date. *Chem. Soc. Rev.*, ***41***, 370–412 (2012). c) Schmidbaur, H; Schier, A. Argentophilic Interactions. *Angew. Chem., Int. Ed.*, ***54***, 746-784, (2015)

(3) Donamaria, R.; Gimeno, M. C.; Lippolis, V.; López-de-Luzuriaga, J. M.; Monge, M.; Olmos, M. E. Tuning the Luminiscent Properties of a Ag/Au Tetranuclear Complex Featuring Metallophilic Interactions via Solvent-Dependent Structural Isomerization. *Inorg. Chem.*, ***55***, 11299–11310 (2016).

(4) Roundhill, D. M. Photochemistry and Photophysics of Metal Complexes, (Plenum Press: New York and London, 1994) pp. 122–124.

(5) Roundhill, D. M.; Fackler Jr., J. P. Optoelectronic Properties of Inorganic Compounds, (Plenum Press: New York, 1999) p. 254.

(6) Coker, N. L.; Krause Bauer, J. A.; Elder, R. C. Emission Energy Correlates with Inverse of Gold-Gold Distance for Various $[Au(SCN)_2]^-$ Salts, *J. Am. Chem. Soc.*, ***126***, 12–13 (2004).

(7) Baranyai, P.; Marsi, G.; Hamza, A.; Jobbágy, C.; Deák, A. Structural characterization of dinuclear gold(I) diphosphine complexes with anion-triggered luminescence, *Struct. Chem.*, ***26***, 1377-1387 (2015).

(8) Elbjeirami, O.; Omary, M. A.; Stenderb, M.; Balch, A. L. Anomalous structure–luminescence relationship in phosphorescent gold(I) isonitrile neutral complexes, *Dalton Trans.*, 3173–3175 (2004).

(9) Elbjeirami, O.; Gonser, M. W. A.; Stewart, B. N.; Bruce, A. E.; Bruce, M. R. M.; Cundari, T. R.; Omary, M. A. Luminescence, structural, and bonding trends upon varying the halogen in isostructural aurophilic dimers, *Dalton Trans.*, 1522–1533 (2009).

(10) Hiraga, T.; Uchida, T.; Kitamura, N.; Kim, H.-B.; Tazuke, S.; Yagi, T. Excited-State Properties of a Diplatinum(II) Complex under High Pressure, *J. Am. Chem. Soc.*, ***111***, 7466–7469 (1989).

(11) Bar, L.; Englmeier, H.; Gliemann, G.; Klement, U.; Range, K.-J. Luminescence at High Pressures and Magnetic Fields and the Structure of Single-Crystal Platinum(II) Binuclear Complexes $M_x[Pt_2(POP)_4]\cdot nH_2O$ (M_x=Ba_2, $[NH_4]_4$; POP = $P_2O_5H_2^{2-}$), *Inorg. Chem.*, ***29***, 1162–1168 (1990).

(12) Stock, M.; Yersin, H. Polarized Emission from $Ba[Pt(CN)_4]\cdot H_2O$ Single Crystals under High Pressure, *Chem. Phys. Lett.*, ***40(3)***, 423–428 (1976).

(13) Yersin, H.; Gliemann, G. Spectroscopic Studies of $M_x[Pt(CN)_4]_y\cdot H_2O$, *Annals New York Academy of Sciences*, 539–559 (1978).

(14) Yersin, H.; Riedl, U. Extreme Pressure-Induced Shifts of Emission Energies in $M[Au(CN)_2]$ and $M_2[Pt(CN)_4]\cdot nH_2O$. Compounds with Low-Dimensional Metal-Metal Interactions, *Inorg. Chem.*, ***34***, 1642–1645 (1995).

(15) Fischer, P.; Mesot, J.; Lucas, B.; Ludi, A.; Patterson, H.; Hewat, A. Pressure Dependence Investigation of the Low-Temperature Structure of $TlAu(CN)_2$ by High-Resolution Neutron Powder Diffraction and Optical Studies, *Inorg. Chem.*, ***36***, 2791–2794 (1997).

(16) Strasser, J.; Yersin, H.; Patterson, H. H. Effect of high pressure on the emission spectrum of single crystals of $Tl[Au(CN)_2]$, *Chem. Phys. Lett.*, ***295***, 95–98 (1998).

(17) Baril-Robert, F.; Radtke, M. A.; Reber, C. Pressure-Dependent Luminescence Properties of Gold(I) and Silver(I) Dithiocarbamate Compounds, *J. Phys. Chem. C*, ***116***, 2192–2197 (2012).

(18) Woodall, C. H.; Fuertes, S.; Beavers, C. M.; Hatcher, L. E.; Parlett, A.; Shepherd, H. J.; Christensen, J.; Teat, S. J.; Intissar, M.; Rodrigue-Witchel, A.; Suffren, Y.; Reber, C.; Hendon, C. H.; Tiana, D.; Walsh, A.; Raithby, P. R. Tunable Trimers: Using Temperature and Pressure to Control Luminescent Emission in Gold(I) Pyrazolate-Based Trimers, *Chem. Eur. J.*, ***20***, 16933–16942 (2014).

(19) O'Connor, A. E.; Mirzadeh, N.; Bhargava, S. K.; Easun, T. L.; Schröeder, M.; Blake, A. J. Aurophilicity under pressure: a combined crystallographic and *in situ* spectroscopic study. *Chem. Commun*. ***52***, 6769–6772 (2016).

(20) Álvarez, S. Covalent radii revisited. *Dalton Trans*. 2832–2838 (2008).

(21) Citroni, M.; Bini, R.; Foggi, P.; Schettino, V. Role of excited electronic states in the high-pressure amorphization of benzene, *Proc. Natl. Acad. Sci*., ***105***, 7658–7663 (2008).

(22) Forman, R. A.; Permarini, G. J.; Barnett, J. D.; Block, S. Pressure measurement made by the utilization of ruby sharp-line luminescence. *Science*, ***176***, 284–285 (1972).

(23) Oxford Diffraction (**2008-2015**). *CrysAlisPRO*, Oxford Diffraction Ltd, Yarnton, Oxford, England, UK.

(24) Bruker **2001**, *SADABS* (Version 2008/1). Bruker AXS Inc., Madison, Wisconsin, USA.

(25) Dolomanov, O. V.; Bourhis, L. J.; Gildea, R. J.; Howard, J. A. K.; Puschmann, H. OLEX2: a complete structure solution, refinement and analysis program. *J. App. Crystallogr*. ***42***, 339–341 (2009).

(26) Sheldrick G. M. *Acta Crystallogr., Sect A* ***64***, 112–122 (2008).

(27) Gaussian 09, Revision **A.1**, Frisch, M. J.; Trucks, G. W.; Schlgel, H. B.; Scuseria, G. E.;Robb, M. A.; Cheeseman, J. R.; Scalmani, G.; Barone, V.; Mennucci, B.; Petersson, G. A.; Nakatsuji, H.; Caricato, M.; Li, X.; Hratchian, H. P.; Izmaylov, A. F.; Bloino, J.; Zheng, G.; Sonnenberg, J. L.; Hada, M.; Ehara, M.; Toyota, K.; Fukuda, R.; Hasegawa, J.; Ishida, M.; Nakajima, T.; Honda, Y.; Kitao, O.; Nakai, H.; Vreven, T.; Montgomery, J. A., Jr.; Peralta, J. E.;

Ogliaro, F.; Bearpark, M.; Heyd, J. J.; Brothers, E.; Kudin, K. N.; Staroverov, V. N.; Kobayashi, R.; Normand, J.; Raghavachari, K.; Rendell, A.; Burant, J. C.; Iyengar, S. S.; Tomasi, J.; Cossi, M.; Rega, N.; Millam, J. M.; Klene, M.; Knox, J. E.; Cross, J. B.; Bakken, V.; Adamo, C.; Jaramillo, J.; Gomperts, R.; Stratmann, R. E.; Yazyev, O.; Austin, A. J.; Cammi, R.; Pomelli, C.; Ochterski, J. W.; Martin, R. L.; Morokuma, K.; Zakrzewski, V. G.; Voth, G. A.; Salvador, P.; Dannenberg, J. J.; Dapprich, S.; Daniels, A. D.; Farkas, O.; Foresman, J. B.; Ortiz, J. V.; Cioslowski, J.; Fox, D. J. Gaussian, Inc., Wallingford CT (2009).

(28) Adamo, C.; Barone, V. Toward reliable density functional methods without adjustable parameters: The PBE0 model *J. Chem. Phys.*, **1999**, 110, 6158-6171.

(29) Andrae, D.; Haeussermann, U.; Dolg, M.; Stoll, H.; Preuss, H.; Energy-adjusted *ab initio* pseudopotentials for the second and third row transition elements *Theor. Chim. Acta*, **1990**, **77**, 123-141.

(30) Bergner, A.; Dolg, M.; Küchle, W.; Stoll, H.; Preuss, H. Ab initio energy-adjusted pseudopotentials for elements of groups 13–17 *Mol. Phys.*, **1993**, 80, 1431-1441.

(31) Huzinaga, S. *Gaussian Basis Sets for Molecular Calculations*; Elsevier: Amsterdam, **1984**, p16.

(32) Huzinaga, S. Gaussian- Type Functions for Polyatomic Systems. I *J. Chem. Phys.*, **1965**, 42, 1293-1302.